

Heat Transfer Analysis for Endothermic Reacting Fluids

Hiroyuki Kimura*

Division of Production and Information Systems Engineering, Muroran Institute of Technology
 27-1, Mizumoto, Muroran, Hokkaido 050-8585, Japan
 s1122181@mmm.muroran-it.ac.jp

Keywords: Endothermic Fuels, Regenerative Cooling, Convective Heat Transfer

Abstract

Endothermic fuels are known as a probable fuel for hypersonic atmospheric flight vehicles and advanced propulsion systems, as well as cryogenic fuels. Especially, from the standpoint of the advanced regenerative cooling use, they are quite useful as a coolant fuel because of their large heat sink due to their chemical decompositions; so-called endothermic cooling effect. However, no heat transfer equations have been proposed taking into account such endothermic reactive behaviors concretely. This paper describes an analytical method for evaluation of the heat transfer rates between endothermic reacting coolant fuel and coolant-side wall in the regenerative cooling passages. Heat transfer mechanism is indicated based on a classical transport-phenomenological approach. A new relational expression of Nusselt number ratio for forced-convective heat transfer with such endothermic reactions is also proposed by theoretical approaches using some classical hypotheses. Its applicability is assessed provisionally by comparison with confirmed results of heated tube tests for supercritical JP-7 fuel carried out at NASA Lewis Research Center, using its heat sink characteristics evaluated by United Technologies Research Center (UTRC). As a result, it has been suggested that the proposed relational equation is applicable to the evaluation of enhancement of Nusselt numbers due to such reactions in developed turbulent flows such as in the regenerative cooling passages.

Introduction

To achieve the practical use of hypersonic atmospheric flight vehicles and advanced propulsion systems for them, it is necessary to develop effective cooling technologies against some associated thermal issues; e.g. aerodynamic heating on the body surface, high heat load inside the combustion chamber. Endothermic fuels—storable hydrocarbon fuels, such as JP-7, JP-8+100, methylcyclohexane etc.—are known as a probable fuel for such vehicle systems as well as cryogenic fuels. They can augment their heat sink capabilities due to decompositions of the fuel molecules at high-temperatures generally over 900 K⁽¹⁾⁻⁵⁾.

Figure 1 shows some confirmed enhanced total heat sink capabilities of typical hydrocarbon fuels evaluated by Huang et al. at UTRC⁶⁾. Physical (i.e.

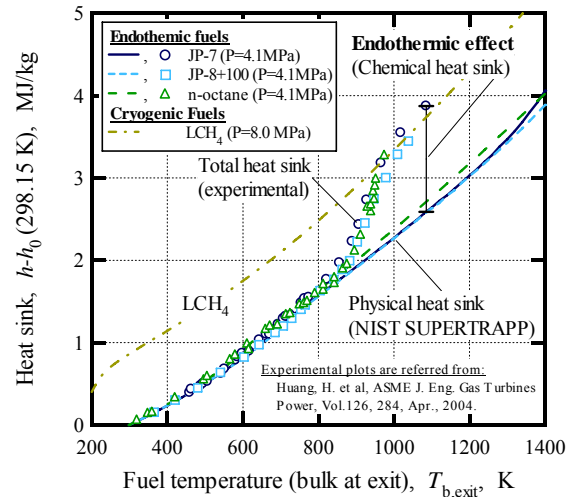


Fig. 1 Heat sink capabilities of endothermic fuels (JP-7, JP-8+100, and n-octane); comparing to the sensible heat sink capability of cryogenic LCH₄.

sensible) heat sink curves, namely without chemical heat sink effects, of the hydrocarbon fuels and cryogenic LCH₄ were estimated using NIST SUPERTRAPP⁷⁾. Figure 1 indicates also that the enhanced total heat sink capabilities of the hydrocarbon fuels due to their chemical decompositions are comparable to that of the cryogenic LCH₄.

One of the problems, to be solved for a practical use of such endothermic fuels into the advanced regenerative cooling system technologies, is to investigate their heat transfer characteristics enhanced due to their large heat sink effects. However, currently, no heat transfer equations have been proposed taking into account their chemical decomposition behaviors concretely; except experimental correlation methods such as property ratio method, reference temperature method⁽⁸⁾⁻¹⁰⁾, etc. for some particular jet or rocket fuels.

In this paper, an analytical method is proposed for evaluation of the improved heat transfer rates between endothermic reacting coolant fuel and coolant-side wall such as in the regenerative cooling passages for advanced future hypersonic propulsions. Heat transfer mechanisms which involved endothermic reactive behaviors are described based on a classical transport-phenomenological approach. In this theoretical approach, a new state-variable—extent of reaction—is introduced for the description of chemically-related insensible heats. A new rational expression equation of Nusselt number ratio is derived; it denotes the ratio

* Doctoral student.

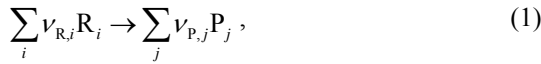
of heat fluxes (or ratio of heat transfer coefficients) with to without endothermic reactions.

A Theory for Heat Transfer Related to Endothermic Reactions

For the regenerative cooling use of endothermic cooling effect as mentioned above, chemical decompositions are induced due to high heat loads from the high temperature combustor walls. Then, it is considered the reaction which occurs in the coolant passage as heterogeneous reaction; not uniformly-reacting homogeneous reaction. Therefore, hereinafter, the reactions are treated as the former.

Reaction Model: Introduction of the Extent of Reaction

Consider a generalized overall reaction equation for an arbitrary chemical decomposition reaction of mixtures as follows:



where, R_i is reactant component, P_i is product component which is decomposed due to advancement of the reaction. Then, $\nu_{R,i}$ and $\nu_{P,j}$ are stoichiometric coefficients of the corresponding reactant and product components respectively. According to Hess's law, amount of the heat of reaction in Eq. (1) is not depends on its reaction paths or its intermediate products. Particularly, if the reactant is one-component, Eq. (1) can be written as:



For the chemical reaction as denoted in Eq. (1), the stoichiometric relation expression is defined as:

$$d\xi \equiv \frac{dN_{R,1}}{-\nu_{R,1}} = \frac{dN_{R,2}}{-\nu_{R,2}} = \dots = \frac{dN_{R,i}}{-\nu_{R,i}} = \dots = \frac{dN_{R,n}}{-\nu_{R,n}} \\ = \frac{dN_{P,1}}{\nu_{P,1}} = \frac{dN_{P,2}}{\nu_{P,2}} = \dots = \frac{dN_{P,j}}{\nu_{P,j}} = \dots = \frac{dN_{P,m}}{\nu_{P,m}}, \quad (2)$$

where, $dN_{R,i}$ and $dN_{P,j}$ are amount of change in number of moles of the corresponding reactants and products, respectively. Then $d\xi$ is the amount of change in the extent of reaction for the overall reaction; a state variable for chemically reacting systems defined by de Donder. The extent of reaction $d\xi$ represents the amount of changes in number of moles of the all components which participates in the chemical reaction¹¹⁾.

Due to introduction of the extent of reaction ξ as above, specific enthalpy for chemically reacting fluid is represented as a function of its temperature T and ξ , as $h = h(T, \xi)$ in a constant pressure system. Therefore, amount of change in the specific enthalpy of the fluid due to advancement of chemical reaction is proportional to the amount of change in the extent of reaction as $dh_{\text{chem}} = h_{p,T} d\xi$. Here, $h_{p,T}$ is chemical specific heat, defined as $h_{p,T} \equiv (\partial h / \partial \xi)_{p,T}$ ¹¹⁾ for a constant pressure and temperature system. It denotes the rate of change in chemical enthalpy—i.e. the heat of reaction—per unit extent of reaction for a constant

pressure and temperature system. As well as physical specific heat $c_{p,\xi}$ —a rate of change in physical enthalpy per unit temperature—is defined as $c_{p,\xi} \equiv (\partial h / \partial T)_{p,\xi}$ in a partial differential form for a constant pressure and extent of reaction system. The specific heats $h_{p,T}$ and $c_{p,\xi}$ denote also the enthalpy/energy densities due to their definitions. The extent of reaction ξ denotes a degree of change in insensible chemical heat of reaction; as well as the temperature denotes a degree of sensible physical heat which is measurable by using such as thermometers.

Definition of the Nusselt Number Ratio

According to previously reported results of heated tube tests using some hydrocarbon fuels, e.g. the tests carried out at NASA Lewis Research Center using JP-7¹²⁾ etc., it has been confirmed that the overall heat flux which convected into the fuels from high-temperature wall is enlarged due to their chemical decompositions.

First of all, consider a forced-convective flow along a high-temperature wall as shown in Fig. 2. Here, for the description of the enhanced overall heat flux, increment of heat flux related to the decomposition of the fuels is defined as q_y^{chem} ; it is allowed due to the above-mentioned confirmed fact. Then, the overall heat flux q_y^{total} is expressed as:

$$q_y^{\text{total}} = -\lambda \frac{\partial T}{\partial y} + q_y^{\text{chem}}, \quad (3)$$

where, first part of the right-hand-side is the local heat flux convected into the fuels as a thermally-related heat flux q_y^{phys} ; it is denoted by the Fourier's law of heat conduction. Here, λ is molecular thermal conductivity of the fuel, and $\partial T / \partial y$ is the temperature gradient in the direction of the heat flow.

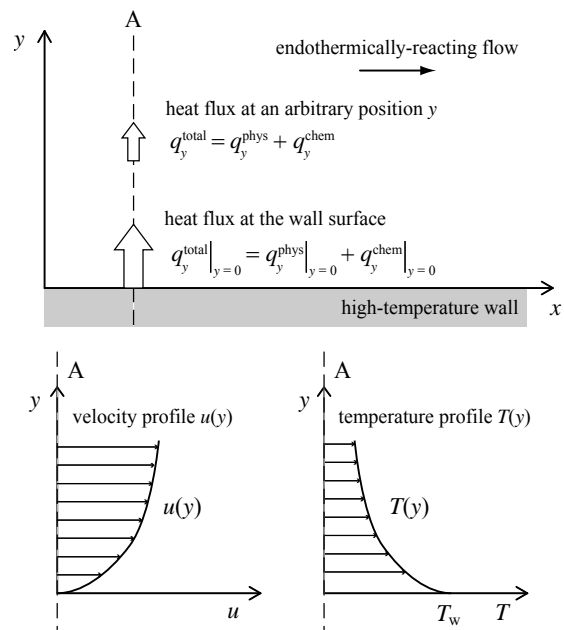


Fig. 2 Overall heat fluxes convected into the endothermically-reacting flow along a high-temperature wall.

From the definition of the Nusselt number—the ratio of the convective heat flux at the wall surface to the molecular heat conduction of the fluid—, Nusselt number ratio $Nu^* = Nu_{total}/Nu_{phys}$ which denotes the ratio of convective flows with to without decompositions is described as:

$$Nu^* = \frac{Nu_{total}}{Nu_{phys}} = \frac{\alpha_{total}}{\alpha_{phys}} = \frac{q_y^{total}|_{y=0}}{q_y^{phys}|_{y=0}} = 1 + \frac{q_y^{chem}|_{y=0}}{q_y^{phys}|_{y=0}} \quad (4)$$

where, α_{total} and α_{phys} are heat transfer coefficients with and without the decompositions respectively. Here, they are defined as due to the Newton's law of cooling:

$$q_y^{total} = \alpha_{total} \Delta T_w, \quad (5)$$

$$q_y^{phys} = \alpha_{phys} \Delta T_w, \quad (6)$$

where, ΔT_w is a temperature difference between the wall temperature T_w and the reference temperature T_{ref} of the fluid. Eq. (4) denotes that the non-dimensionalized Nusselt number Nu^* equals to the ratio of heat transfer coefficients α_{total} to α_{phys} as well as to the ratio of heat fluxes at the wall surface $q_y^{total}|_{y=0}$ to $q_y^{phys}|_{y=0}$.

A Description of the Enhanced Local Heat Flux due to Endothermic reactions

According to the transition-state theory—or the extremum principle for thermodynamic potentials—, advancement of chemical reaction requires the addition of energy from external energy source, as well as its temperature rise also requires that. In other words, substances at equilibrium in an adiabatic system do not advance the reactions or not raise the temperature by themselves.

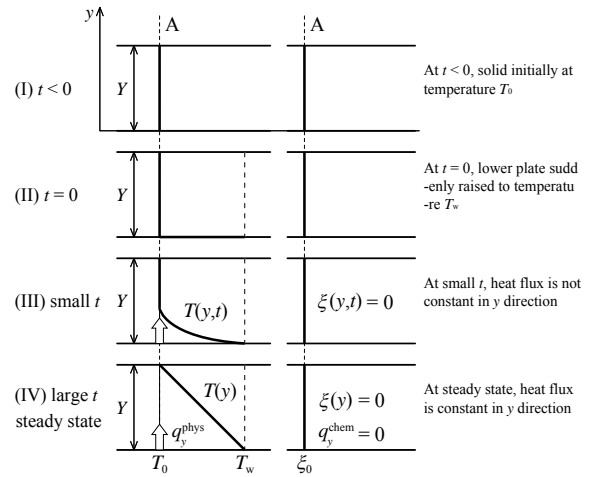
For the description of the enhanced heat flux due to endothermic reaction, here consider a thin slab of solid material of area A located between two parallel plates as shown in Figure 3; based on the description of the Fourier's law of heat conduction by Bird et al.¹³⁾ Here, it is assumed that the upper plate is adiabatic wall.

Figure 3 (a) shows the development process of the profiles of the temperature T and the extent of reaction ξ without any chemical reactions. In this case, due to chemical reactions are not advanced, the extent of reaction profiles is not created; that is, $\xi = 0$ constantly. Hence, the heat flux through the slab in this case is described by Fourier's law of heat conduction; that is, $q_y^{chem} = 0$ in Eq. (3).

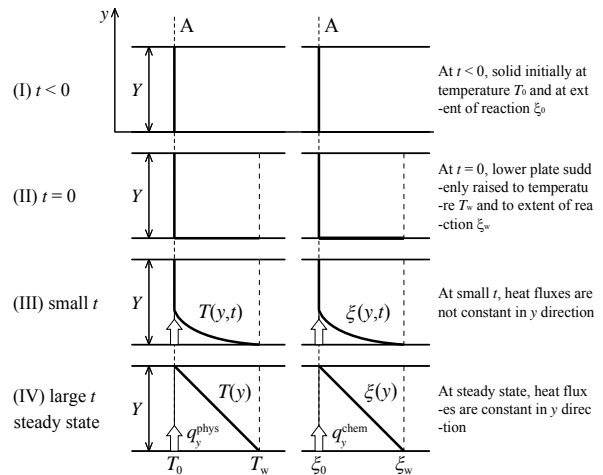
Then, Fig. 3 (b) shows the development process of the profiles of the temperature T and the extent of reaction ξ with endothermic reactions. Imagine that:

(I) Initially, for time $t < 0$, the slab is at temperature T_0 and at extent of reaction $\xi_0 = 0$ throughout.

(II) At $t = 0$, the lower plate is suddenly brought to a slightly higher temperature T_w and maintained at that temperature constantly. At the same time, the slab temperature at $y = 0$ —the position that the slab molecules contact with the lower plate—is brought to the temperature T_w . Furthermore, if the temperature T_w exceeds the reactive transition-state temperature of the slab molecules, the extent of reaction is also brought



(a) Profiles without any chemical reactions.



(b) Profiles with endothermic reactions.

Fig. 3 Development processes of the temperature profile and extent of reaction profile for a solid substance between two parallel plates; adiabatic and non-adiabatic walls.

to the extent of reaction ξ_w ; an attainable extent of reaction which is determined by the lower plate temperature T_w .

(III) As time proceeds, the profiles of temperature T and extent of reaction ξ in the slab changes. The extent of reaction $\xi(y)$ at an arbitrary y position is also determined by the temperature $T(y)$ at the correspondent position.

(IV) Ultimately, linear steady-state distributions of temperature $T(y)$ and extent of reaction $\xi(y)$ are attained, as shown in Fig. 3 (b).

When this steady-state condition has been reached, constant rates of heat flow Q_y^{phys} and Q_y^{chem} through the slab is required to maintain the temperature difference $\Delta T = T_w - T_0$ and the extent of reaction distance $\Delta \xi = \xi_w - \xi_0$. It is found then that for sufficiently small values of ΔT and $\Delta \xi$, the following relation holds:

$$\frac{Q_y^{\text{phys}}}{A} = \lambda \cdot \frac{\Delta T}{Y}, \quad (7)$$

$$\frac{Q_y^{\text{chem}}}{A} = \kappa \cdot \frac{\Delta \xi}{Y}, \quad (8)$$

that is, the rates of heat flow per unit area A are proportional to the temperature decrease and the extent of reaction decrease over the distance Y . Here, a new constant of proportionality κ is defined as thermal conductivity of the slab related to the advancement of endothermic reactions. The total heat flow through the slab Q_y^{total} is sum of the heat flows Q_y^{phys} and Q_y^{chem} . For description of the limiting form of Eq. (7) and (8), it is assumed that the slab thickness approaches zero. That is, the local rates of heat flow per unit area—namely, heat fluxes—in the positive y direction are described as:

$$q_y^{\text{phys}} = -\lambda \cdot \frac{\partial T}{\partial y}, \quad (9)$$

$$q_y^{\text{chem}} = -\kappa \cdot \frac{\partial \xi}{\partial y}, \quad (10)$$

therefore, the overall heat flux q_y^{total} , sum of the heat fluxes of q_y^{phys} and q_y^{chem} , is described as:

$$q_y^{\text{total}} = -\lambda \cdot \frac{\partial T}{\partial y} - \kappa \cdot \frac{\partial \xi}{\partial y}, \quad (11)$$

where, the second part of the right-hand-side denotes the chemical heat flux related to the development of extent of reaction profile; as well as the first part of that is the physical heat flux related to the development of temperature profile as denoted by Fourier's law of heat conduction. That is, it is the heat flux related to endothermic chemical decompositions.

In above description, for the derivation of steady-state heat flow mechanisms, it is assumed that the local reaction rate of the slab molecules is infinity $\partial \xi / \partial t \rightarrow \infty$; i.e. slab molecules at arbitrary positions are in local equilibrium. It is also assumed that the extent of reaction $\xi(y)$ is a proportional function of temperature $T(y)$.

Important: Temperature gradient/profile is induced due to heat flux from the external heat/energy source; not the heat flux is induced due to temperature gradient. In other words, temperature gradient is not formed without the heat flow in the steady-state condition. Hence, it is also that extent of reaction gradient is induced due to heat flux from the external heat source; i.e. from the high-temperature wall in this case. Additionally, in a convective boundary layer, temperature and extent of reaction gradients are induced due to heat flux from the external heat source and/or due to the convective flow which reduces the heat of fluid by convection.

Derivation of the Nusselt Number Ratio for General Forced-Convective Flows with Endothermic Reactions

Consider a general forced-convective flow with endothermic reaction due to its chemical decompositions, with three profiles of state-variables as shown in Figure 4. Here, the following assumptions

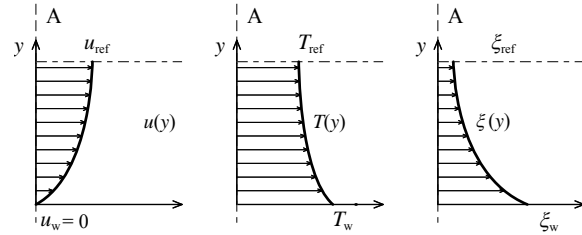


Fig. 4 General profiles of velocity $u(y)$, temperature $T(y)$, and extent of reaction $\xi(y)$ in laminar forced-convective flow with endothermic reactions along a high-temperature wall.

are introduced: Fluid pressure p is constant in the y direction. Specific heats of the fluid, $c_{p,\xi}$ and $h_{p,T}$, are constant in the y direction. Transport properties of the fluid, μ , λ , and κ , are constant in the y direction.

According to Eq. (11), the total heat flux through the fluid in the y direction is written as:

$$q_y^{\text{total}} = -\left(1 + \frac{\kappa}{\lambda} \cdot \frac{\partial \xi}{\partial T}\right) \cdot \lambda \cdot \frac{\partial T}{\partial y}, \quad (12)$$

where, $\partial \xi / \partial T$ denotes the ratio of the extent of reaction gradient to the temperature gradient at an arbitrary position y .

For the derivation of the Nusselt number ratio, it is to know is the heat flux at the wall surface ($y = 0$); due to definition of the Nusselt number. From the Eq. (12) and (9), the heat fluxes at the wall surface with and without chemical decompositions are written as:

$$q_y^{\text{total}}|_{y=0} = -\left(1 + \frac{\kappa}{\lambda} \cdot \frac{\partial \xi}{\partial T}\right) \cdot \lambda \cdot \frac{\partial T}{\partial y}\bigg|_{y=0}, \quad (13)$$

$$q_y^{\text{phys}}|_{y=0} = -\lambda \cdot \frac{\partial T}{\partial y}\bigg|_{y=0}, \quad (14)$$

substituting Eq. (13) and (14) into Eq. (4), then the Nusselt number ratio Nu^* is derived as:

$$Nu^* = 1 + \frac{\kappa}{\lambda} \cdot \frac{\partial \xi}{\partial T}\bigg|_{y=0}, \quad (15)$$

where, the second part of the right-hand-side denotes the enhancement of the Nusselt number related to endothermic reactions.

When non-dimensional temperature T^* and non-dimensional extent of reaction ξ^* are defined as:

$$T^* \equiv \frac{\Delta T}{\Delta T_w} = \frac{T - T_{\text{ref}}}{T_w - T_{\text{ref}}}, \quad (16)$$

$$\xi^* \equiv \frac{\Delta \xi}{\Delta \xi_w} = \frac{\xi - \xi_{\text{ref}}}{\xi_w - \xi_{\text{ref}}}, \quad (17)$$

then, from the description of Eq. (15), the relation expression of the Nusselt number ratio for general forced-convective flow with endothermic reaction is derived as:

$$Nu^* = 1 + \frac{\text{Pr}}{\text{Ki}} \cdot \frac{\partial \xi^*}{\partial T^*}\bigg|_{y=0} \cdot \frac{\Delta h_{\text{chem},w}}{\Delta h_{\text{phys},w}}, \quad (18)$$

where, Pr is molecular Prandtl number. Then, Ki is tentative non-dimensional number defined as $Ki \equiv$

$\mu/(\kappa/h_{p,T})$; the latter denotes the ratio of kinetic viscosity coefficient ν ($\equiv \mu/\rho$) to chemico-thermal diffusivity a_κ ($\equiv \kappa/\rho h_{p,T}$), as well as Prandtl number Pr denotes the ratio of kinetic viscosity coefficient ν to physico-thermal diffusivity a_λ ($\equiv \lambda/\rho c_{p,\xi}$). (Or, it should be named as chemical Prandtl number Pr_{chem}). Then, $\partial \xi^*/\partial T^*|_{y=0}$ is the ratio of non-dimensional gradient of extent of reaction $\partial \xi^*/\partial y^*$ to gradient of temperature $\partial T^*/\partial y^*$ at the wall surface. $\Delta h_{chem,w} = h_{p,T} \Delta \xi_w$ is difference of the chemical enthalpy between the extent of reaction at the wall (of wall temperature T_w) and the extent of reaction at the reference position (main stream, bulk, or center-line), as well as $\Delta h_{phys,w} = c_{p,\xi} \Delta T_w$ is difference of the physical enthalpy between the temperature at the wall and the temperature at the reference position (main stream, bulk, or center-line).

From the definitions of non-dimensionalized enthalpy such as:

$$h^* \equiv \frac{\Delta h}{\Delta h_w} = \frac{h - h_{ref}}{h_w - h_{ref}}, \quad (19)$$

then, Eq. (18) is also described as follows:

$$Nu^* = 1 + \frac{Pr}{Ki} \cdot \frac{\partial \xi^*}{\partial T^*} \Big|_{y=0} \cdot \Gamma_p, \quad (20)$$

where, Γ_p is the ratio of non-dimensionalized specific heats $h_{p,T}^*$ to $c_{p,\xi}^*$ with constant pressure; it also denotes the ratio of the differences of chemical enthalpy $\Delta h_{chem,w}$ to physical enthalpy $\Delta h_{phys,w}$. So the definition of Γ_p by the author is:

$$\Gamma_p \equiv \frac{h_{p,T}^*}{c_{p,\xi}^*} = \frac{(\partial h^*/\partial \xi^*)_{p,T}}{(\partial h^*/\partial T^*)_{p,\xi}} = \frac{(\Delta h_{chem,w})_{p,T}}{(\Delta h_{phys,w})_{p,\xi}}. \quad (21)$$

On the other hand, the ratio of specific heat γ_ξ of constant pressure $c_{p,\xi}$ to constant volume $c_{v,\xi}$ is also defined as:

$$\begin{aligned} \gamma_\xi &\equiv \frac{c_{p,\xi}}{c_{v,\xi}} = \frac{(\partial h/\partial T)_{p,\xi}}{(\partial h/\partial T)_{v,\xi}} \\ &= \frac{c_{p,\xi}^*}{c_{v,\xi}^*} = \frac{(\partial h^*/\partial T^*)_{p,\xi}}{(\partial h^*/\partial T^*)_{v,\xi}} = \frac{(\Delta h_{phys,w})_{p,\xi}}{(\Delta h_{phys,w})_{v,\xi}} \equiv \Gamma_\xi, \end{aligned} \quad (22)$$

from this expression of definition of specific ratio of γ_ξ , it can be denoted as therefore the ratio of non-dimensional specific heats with constant extent of reaction.

The relational expression of Eq. (20) may be generally applicable to any forced-convective flow geometries with endothermic reactions; such as flow on a flat plate and flow in a tube, etc. But it should be verified.

Derivation of the Nusselt Number Ratio for Fully Developed Turbulent Forced-Convective Flows with Endothermic Reactions

Fig. 5 shows general profiles of state-variables of velocity $u(y)$, temperature $T(y)$, and extent of reaction $\xi(y)$ in developed turbulent forced-convective flow along a high-temperature wall. In such flow, by analogy with Boussinesq's hypothesis for turbulent

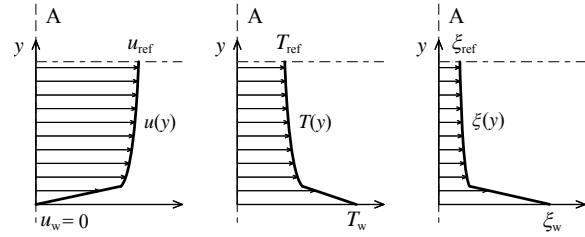


Fig. 5 General profiles of velocity $u(y)$, temperature $T(y)$, and extent of reaction $\xi(y)$ in developed turbulent forced-convective flow with endothermic reactions along a high-temperature wall.

viscosity, the heat flux with endothermic reacting turbulent flow at an arbitrary y position is described as:

$$q_y^{phys} = -\lambda \frac{\partial \bar{T}}{\partial y} + \rho c_{p,\xi} \bar{T} v', \quad (23)$$

$$q_y^{chem} = -\kappa \frac{\partial \bar{\xi}}{\partial y} + \rho h_{p,T} \bar{\xi} v', \quad (24)$$

hence,

$$q_y^{phys} = -(\lambda + \lambda^{turb}) \frac{\partial \bar{T}}{\partial y}, \quad (25)$$

$$q_y^{chem} = -(\kappa + \kappa^{turb}) \frac{\partial \bar{\xi}}{\partial y}, \quad (26)$$

or,

$$q_y^{phys} = -\rho c_{p,\xi} (a_\lambda + a_\lambda^{turb}) \frac{\partial \bar{T}}{\partial y}, \quad (25)'$$

$$q_y^{chem} = -\rho h_{p,T} (a_\kappa + a_\kappa^{turb}) \frac{\partial \bar{\xi}}{\partial y}, \quad (26)'$$

so, from the Eqs. (25) and (26), the total heat flux is described as:

$$q_y^{total} = -(\lambda + \lambda^{turb}) \frac{\partial \bar{T}}{\partial y} - (\kappa + \kappa^{turb}) \frac{\partial \bar{\xi}}{\partial y}, \quad (27)$$

where, the second parts of the right-hand-side of Eqs. (23) and (24) are given by the derived energy equation for turbulent flow with endothermic reaction. For derivation of the energy equation for turbulent flow with endothermic reaction, velocity v , temperature T , and extent of reaction ξ are written as $v = \bar{v} + v'$, $T = \bar{T} + T'$, $\xi = \bar{\xi} + \xi'$; \bar{v} , \bar{T} , and $\bar{\xi}$ are time averages of velocity, temperature, and extent of reaction, respectively. Then v' , T' , and ξ' are turbulent fluctuations of velocity, temperature, and extent of reaction, respectively. For Eqs. (25) and (26), λ and λ^{turb} are the coefficient of molar and turbulent physico-thermal conductivity respectively, then κ and κ^{turb} are the coefficient of molar and turbulent chemico-thermal conductivity respectively. For Eqs. (25)' and (26)', a_λ and a_λ^{turb} are the coefficient of molar and turbulent physico-thermal diffusivity; defined as $\lambda/(\rho c_{p,\xi})$ and $\lambda^{turb}/(\rho c_{p,\xi})$ respectively. Then, a_κ and a_κ^{turb} are the coefficient of molar and turbulent chemico-thermal diffusivity; defined as $\kappa/(\rho h_{p,T})$ and $\kappa^{turb}/(\rho h_{p,T})$ respectively. Detailed descriptions about

the derivation of the turbulent energy equation in y direction and the turbulent heat flux in an arbitrary y position are omitted in this paper.

As mentioned above, for the derivation of Nusselt number ratio, it is to know is the heat flux at the wall surface due to definition of the Nusselt number. Hence, it is not necessary to know the behavior of reacting fluid in the turbulent layer which is away from the wall surface. From this reason, first, consider the behaviors in near-wall layer of the fluid; so-called laminar sub-layer.

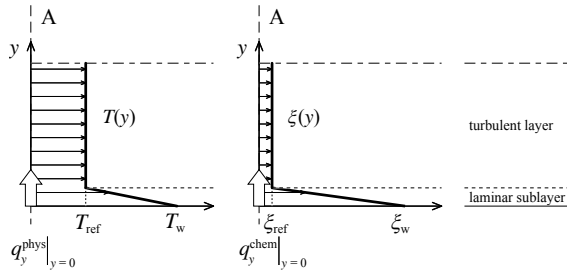
To describe the Nusselt number ratio in a simple form, introductions of some hypothesis for fully developed turbulent forced-convective heat transfer are described in what follows.

(i) Introduction of Hypothesis in the Prandtl's Analogy

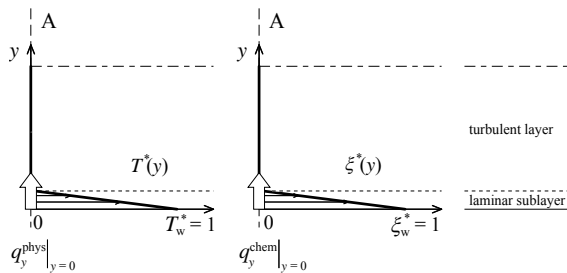
According to hypothesis in the Prandtl's analogy, the heat flux through the laminar sub-layer near the wall is constant; That is, the temperature T is proportional to y coordinate in the layer as shown in Fig. 6 (a). Introducing this hypothesis to the extent of reaction, namely, it can be assumed that the extent of reaction ξ is also proportional to y coordinate in the layer. Then, considering the non-dimensional profiles of temperature T and extent of reaction ξ , as shown in Fig.6 (b), it can be allowable that the introduction of a hypothesis as:

$$\left. \frac{\partial \xi^*}{\partial T^*} \right|_{y=0} \cong 1, \quad (28)$$

hence, the Nusselt number ratio denoted in Eq. (20) is



(a) Dimensional profiles.



(b) Non-dimensionalized profiles.

Fig. 6 Dimensional and non-dimensional profiles of the temperature and extent of reaction in a fully developed turbulent forced-convective flow near the wall surface with endothermic reactions.

approximated as:

$$Nu^* \cong 1 + \frac{Pr}{Ki} \cdot \Gamma_p, \quad (29)$$

(ii) Introduction of Hypothesis in the Reynolds's Analogy

According to the hypothesis in the Reynolds's analogy that excludes the existence of laminar sub-layer; that is, all region is takes without the laminar sub-layer. In other words, it is assumed that the whole region is the turbulent layer. Due to this hypothesis— $a_\lambda \ll a_\lambda^{turb}$ and $a_\kappa \ll a_\kappa^{turb}$ in the near-wall layer—hence the molecular thermal diffusivity coefficients a_λ and a_κ in Eq. (25)' and (26)' are neglected. So the total heat flux at the wall surface with the Reynolds's hypothesis is described as:

$$q_y^{total} \Big|_{y=0} = -\lambda^{turb} \cdot \left. \frac{\partial T}{\partial y} \right|_{y=0} - \kappa^{turb} \cdot \left. \frac{\partial \xi}{\partial y} \right|_{y=0}, \quad (30)$$

hence, the Nusselt number ratio which introduced the Prandtl's hypothesis denoted above is described as (dividing Eq. (30) by the turbulent heat flux without the reaction at $y = 0$):

$$Nu^* \cong 1 + \frac{Pr^{turb}}{Ki^{turb}} \cdot \Gamma_p, \quad (31)$$

where, Pr^{turb} and Ki^{turb} are defined as $v^{turb}/(\lambda^{turb}/(\rho c_{p,\xi}))$ and $v^{turb}/(\kappa^{turb}/(\rho h_{p,T}))$, respectively; v^{turb} is turbulent kinematic viscosity defined as μ^{turb}/ρ .

In addition, due to the other hypothesis in the Reynolds's analogy— $v^{turb} \approx a_\lambda^{turb}$ in turbulent region—it can also be assumed as $v^{turb} \approx a_\kappa^{turb}$; that is, $a_\lambda^{turb} \approx a_\kappa^{turb}$, hence $Pr^{turb} \approx Ki^{turb}$. Therefore, the following approximation is allowed:

$$\frac{Pr^{turb}}{Ki^{turb}} \cong 1. \quad (32)$$

As a result of introductions of hypothesis in the Prandtl's and Reynolds's analogies, ultimately the Nusselt number ratio is approximated as follows:

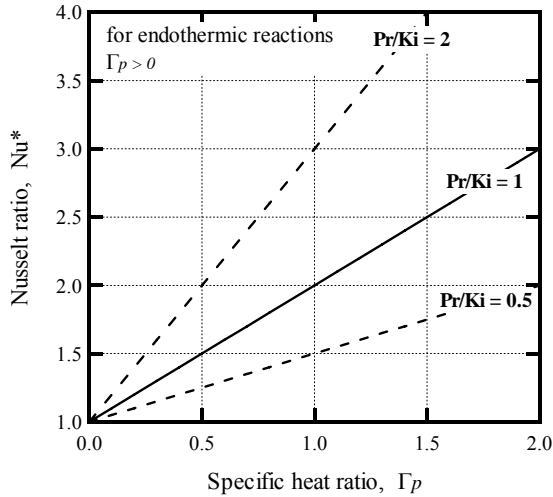
$$Nu^* \cong 1 + \Gamma_p. \quad (33)$$

This relational expression of Nu^* and Γ_p is simple for practical use; it is also in a special case $Pr/Ki = 1$ in Eq. (29) for turbulent flow with laminar sub-layer. This relation for fluids with low-scale Γ_p is indicated in Fig. 7 (a). This expression denotes also Nu^* is approximately equal to Γ_p , i.e. $Nu^* \approx \Gamma_p$, for fluids with high-scale Γ_p as shown in Fig. (b).

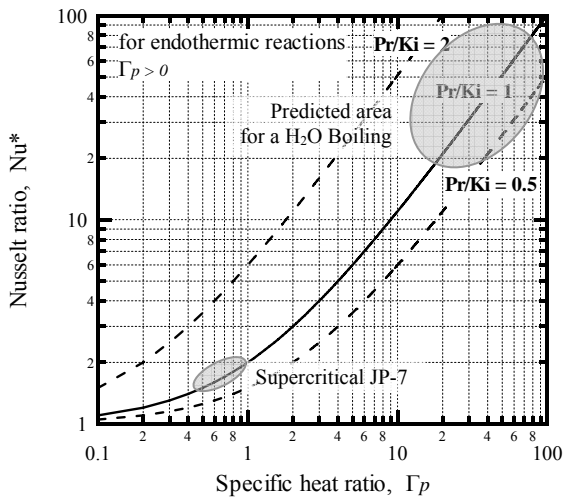
The relation expression of Eq. (29) and (33) may be applicable to any flow, because the Nusselt number depends on only the ratio of heat flux at the wall surface due to its definition. Additionally, it may be also applicable to boiling heat transfer; Fig.7 (b) shows also the tentatively predicted Γ_p for a H₂O boiling heat transfer rate.

Description of the Non-Dimensional Specific Heat Ratio Γ_p

The specific heat ratio Γ_p in Eq. (29) and Eq. (33) is considered as a function of reactant fluid and catalytic



(a) For low-scale specific heat ratio of Γ_p .



(b) For wide-scale specific heat ratio of Γ_p .

Fig. 7 Relations between Nusselt number ratio Nu^* and specific heat ratio of Γ_p in some Pr/Ki ratio cases.

substance of the solid wall as follows:

$$\Gamma_p = \Gamma_p(\text{Reactant, Catalyst}), \quad (34)$$

where, when the endothermic reaction proceeds, Γ_p denotes positive value ($\Gamma_p > 0$) due to its positive heat of reaction. In contrast, when the exothermic reaction proceeds, Γ_p denotes negative value ($\Gamma_p < 0$) due to its negative heat of reaction; based on the definition of Γ_p in Eq. (21). Then, when no reaction proceeds, Γ_p denotes zero ($\Gamma_p = 0$) due to zero heat of reaction; therefore $Nu^* = 1$.

Predicted orders of Γ_p value for some hydrocarbon fuels are tabulated in Table 1. Figure 7 (a) and (b) shows the relations of Nusselt number ratio Nu^* and non-dimensional specific heat Γ_p in some Pr/Ki ratio cases.

Description of Nusselt Number Equation

For fully developed turbulent flow in smooth tubes, the following relation is recommended by Dittus and

Table 1 Predicted orders of non-dimensional specific heat ratio of Γ_p .

n (m)	substance	specific heat ratio, Γ_p
0 (2)	H ₂	0 (w/o dissociation)
1 (4)	CH ₄	≈ 0
small n	C _{n} H _{m}	small Γ_p
large n	C _{n} H _{m}	large Γ_p
$n \approx 12$	JP-7	~ 0.9 (approx., see below)

n = carbon number.

m = hydrogen number.

Boelter¹⁴⁾:

$$Nu_{DB} = 0.023 Re^{0.8} Pr^{0.4}; \text{ for heating} \quad (35)$$

For example, in a case of that the normal Nusselt number—normal denotes with no chemical reaction—of turbulent forced-convective flow is predictable from Dittus-Boelter's correlation equation, the description of enhanced Nusselt number related to the endothermic reaction of the fluid is available as:

$$\begin{aligned} Nu_{total} &= Nu_{DB}(1 + \Gamma_p) \\ &= 0.023 Re^{0.8} Pr^{0.4}(1 + \Gamma_p), \end{aligned} \quad (36)$$

here, Re is the diameter-based Reynolds number. Meanwhile, Pr is molecular Prandtl number denoted above. All properties in Re and Pr are evaluated at the fluid bulk temperature.

Evaluations of Validity and Applicability of the Proposed Relational Expression

To assess the validity and applicability of the proposed relational expression of Eq. (33)—in a special case of $Pr/Ki = 1$ in Eq. (29)—, comparisons of Nusselt numbers with previously confirmed experimental results are discussed in what follows. For the comparison, the heated tube test results using supercritical JP-7 fuel carried out by Linne et al. (TM-107485¹²⁾) at NASA Lewis Research Center is referred. The tests were conducted for the purpose of correcting data concerning the endothermic cooling use of JP-7 fuels for a hypersonic propulsion system; the report anticipates that coolant-side wall temperature may reach approximately 1,250 K in such propulsion system.

(i) Overview of the Heated Tube Tests at NASA (TM-107485)

According to the report TM-107485¹²⁾, the tests was conducted in NASA LRC Heated Tube facility¹⁵⁾ using electrically heated metallic alloy tubes which has 0.095 in. (0.24 cm) of inner diameter, 14 in. (35.5 cm) of heated section length. Operating pressure is 6.9 MPa (Critical pressure and temperature of JP-7 are approximately 1.8 MPa and 677 K respectively). Heat flux is controlled electrically to increase in steps until the desired wall temperature are achieved as shown in Fig. 8. Due to the report, Reynolds number at tube inlet (at ambient temperature) is 5275, and typical Reynolds number at tube exit during a test was 1.4×10^5 . In the two test sections of Section 4 and

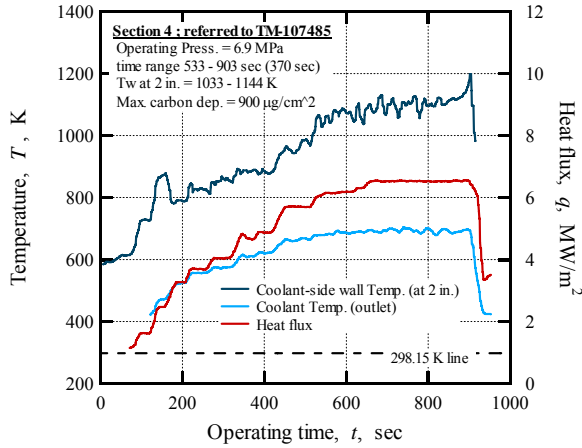


Fig. 8 Histories of temperatures and a heat flux at the heated tube test using endothermic JP-7 fuel (TM-107485¹²); Test Section 4.

Section 5—shown below in Fig.11 (a) to (c), and Fig. 12, respectively—, target coolant-side wall temperatures are 1,030 to 1,145 K, and 1,170 to 1,280 K respectively. Maximum heat fluxed in each test sections are 6.5 MW/m² and 7.4 MW/m² respectively. See the report TM-107485¹² for the other details about the tests.

(ii) Evaluation of Specific Heat Ratio Γ_p and Nusselt Number Ratio Nu^* for supercritical JP-7 fuel

For evaluation of ratio of specific heat Γ_p defined as in Eq. (21), the temperature dependence of chemical heat sink characteristics of supercritical JP-7 evaluated (at a pressure of 4.1 MPa) by Huang et al.⁶ at United Technologies Research Center. Figure 9 shows it as a function of fluid bulk temperature T_b , corresponding to the physical heat sink (i.e. sensible heat sink) characteristics estimated by NIST SUPERTRAPP.

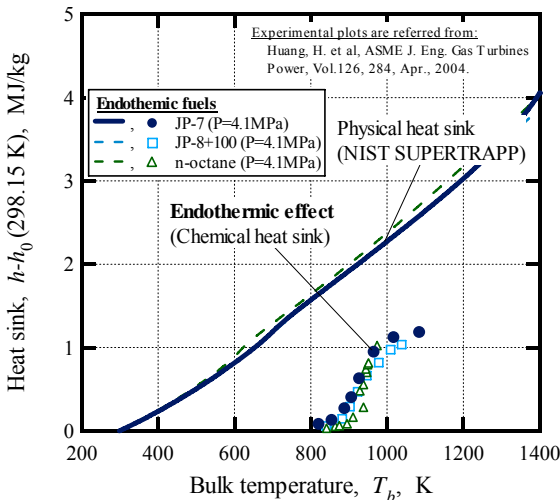


Fig. 9 Evaluated relations between the physical and chemical heat sinks for typical hydrocarbon fuels at supercritical pressure of 4.1 MPa⁶.

Table 2 Predicted values of Γ_p and Nu^* for supercritical JP-7 fuel using the results in TM-107485¹².

(a) For near-inlet conditions.					
	a1	a2	a3	a4	a5
T_b , K	(300)	(350)	(400)	(450)	(500)
T_w , K	1100 ¹²⁾	1100 ¹²⁾	1100 ¹²⁾	1,100 ¹²⁾	1,100 ¹²⁾
$\Delta h_{phys,w}$, MJ/kg	2.64	2.53	2.41	2.28	2.14
$\Delta h_{chem,w}$, MJ/kg	1.32 ⁶⁾	1.32 ⁶⁾	1.32 ⁶⁾	1.32 ⁶⁾	1.32 ⁶⁾
Γ_p at near-inlet	0.50	0.52	0.55	0.58	0.62
Nu^* at near-inlet	1.50	1.52	1.55	1.58	1.62
(b) For near-exit conditions.					
	b1	b2	b3	b4	b5
T_b , K	650 ¹²⁾	650 ¹²⁾	650 ¹²⁾	650 ¹²⁾	650 ¹²⁾
T_w , K	(850)	(900)	(950)	(1000)	(1050)
$\Delta h_{phys,w}$, MJ/kg	0.75	0.93	1.10	1.28	1.47
$\Delta h_{chem,w}$, MJ/kg	0.12 ⁶⁾	0.34 ⁶⁾	0.82 ⁶⁾	1.06 ⁶⁾	1.23 ⁶⁾
Γ_p at near-exit	0.15	0.37	0.74	0.83	0.84
Nu^* at near-exit	1.15	1.37	1.74	1.83	1.84

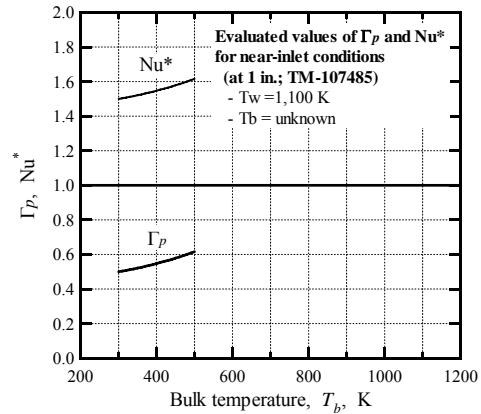
Parenthetic values are presumed unknown values.

T_b = Mean fluid temperature.

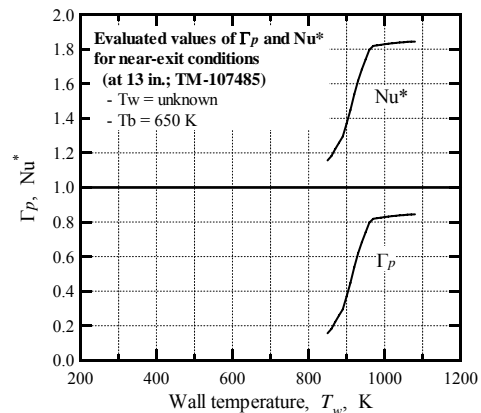
T_w = Coolant-side wall temperature.

$\Delta h_{phys,w}$ = Physical heat sink.

$\Delta h_{chem,w}$ = Chemical heat sink.



(a) For the near-inlet condition (at 1 in.); as a function of unknown fluid temperature of T_b .



(b) For the near-exit condition (at 13 in.); as a function of unknown wall temperature T_w .

Fig. 10 Predicted values of Γ_p and Nu^* for supercritical JP-7 fuel using the reported experimental results of heated tests of TM-107485¹².

The values of Γ_p and Nu^* evaluated due to near inlet (at 1 in. of total heated length of 14 in.) conditions are tabulated in Table 2 (a). Here, the fluid bulk temperature data is not available in TM-107485. Hence the Γ_p and Nu^* values are indicated as a function of the unknown fluid bulk temperature of T_b , as shown in Fig. 10 (a). On the other hand, the values of Γ_p and Nu^* evaluated due to near-exit (at 13 in. of total heated length of 14 in.) conditions are tabulated in Table 2 (b). Here, the wall temperature data is not available in TM-107485. Hence the Γ_p and Nu^* values are indicated as a function of the unknown wall temperature of T_w , as shown in Fig. 10 (b). The near-inlet condition, which indicates a large difference between the wall and fluid bulk temperature, denotes stable Γ_p values of 0.50 to 0.62. On the other hand, the near-exit condition, which indicates a relatively small difference between the wall and fluid bulk temperature, denotes unstable Γ_p values of 0.15 to 0.74 at lower wall temperature. However, it denotes stable Γ_p values of 0.74 to 0.84 at higher wall temperature over 950 K.

(iii) Evaluation and Comparison of the Enhanced Nusselt Numbers

According to TM-107485¹²⁾, a consistent feature was determined that the experimental Nusselt numbers in the beginning—without chemical decompositions due to low heat fluxes—of every test most closely resembled the Dittus-Boelter’s correlation of Eq. (35). It is confirmed also in the following Figs. 11 (a) to (c) and 12; before 160 sec of operating time of the test Section 4 as shown in Fig. 11 (a) to (c); before 60 sec

of operating time of the test Section 5 as shown in Fig. 12. That is, this fact represent that Nusselt numbers of supercritical JP-7 fuel without chemical decompositions can be predicted by the Dittus-Boelter’s correlation equation with comparatively high accuracy. Therefore, this fact allows that the Nu_{phys} is substituted by the Nusselt number Nu_{DB} in Eq. (33)—as denoted in Eq. (36)—for evaluation of Nu_{total} values.

Figure 11 and 12 indicates the comparison results of Nusselt numbers; evaluated by experimental, Dittus-Boelter’s correlation, Sieder-Tate’s correlation, and the proposed correlation ($Nu_{total} = Nu_{DB}(1+\Gamma_p)$) denoted in Eq. (36) due to confirmed consistent features mentioned above). Corresponding temperature histories and heat flux history (at the beginning of chemical decomposition) of Section 4 are indicated above in Fig. 8 for reference. In these figures, fluctuation of experimental Nusselt number curves are not reproduced strictly; mean values are plotted in these figures. See TM-107485 for original experimental curve with fluctuations due to chemical decompositions.

Fig. 11 (a) indicates the Nusselt number curves at 1 in. (near-inlet) of total heated length of 14 in. in Section 4. From these curves, it is confirmed that after the decomposition occurs at 160 sec, the Nusselt number curve which evaluated by the proposed relation due to near-inlet condition ($Nu^* = 1.55$) well accorded with the experimental Nusselt number curve from beginning to end, as well as Sieder-Tate’s correlation curve.

Fig. 11 (b) indicates the curves at 9 in. of total heated length in Section 4. These curves represents

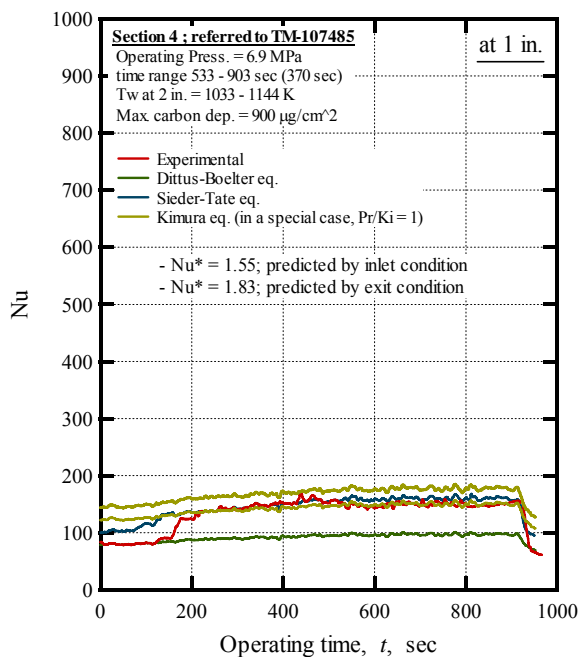


Fig. 11 (a) The comparison result of overall Nusselt numbers between experimental value (TM-107485¹²⁾) and some correlated equation values; Test Section 4: Haynes 230, at 1 in. (near inlet) of total heat length of 13 in.

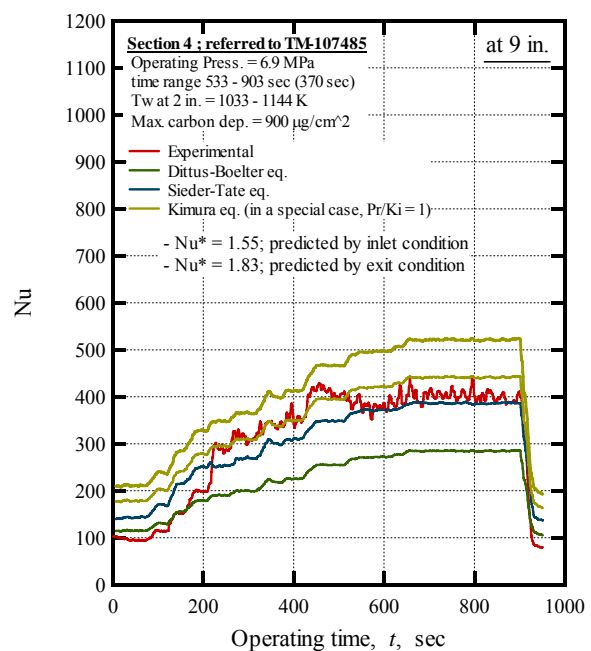


Fig. 11 (b) The comparison result of overall Nusselt numbers between experimental value (TM-107485¹²⁾) and some correlated equation values; Test Section 4: Haynes 230, at 9 in. of total heat length of 13 in.

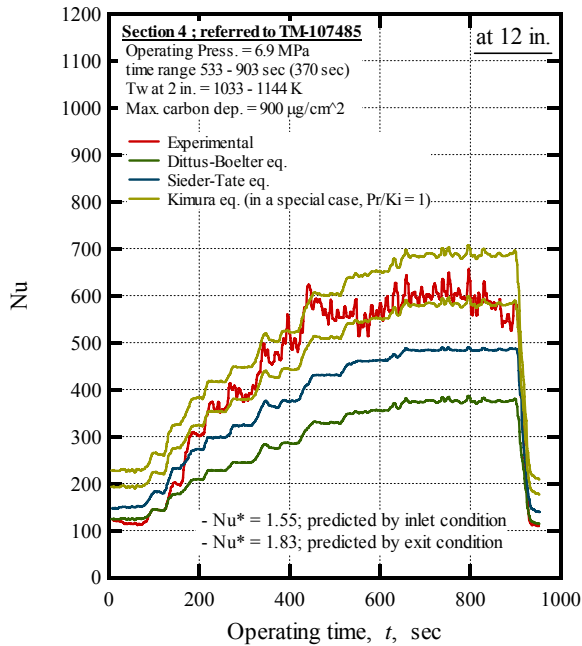


Fig. 11 (c) The comparison result of overall Nusselt numbers between experimental value (TM-107485¹²⁾) and some correlated equation values; Test Section 4: Haynes 230, at 12 in. (near-exit) of total heat length of 14 in.

also that the curve which evaluated by the proposed relation due to near-inlet condition ($Nu^* = 1.55$) will accorded with the experimental curve when chemical decomposition occurs, though Sieder-Tate's correlation curve is no longer accorded with that. After coking formation occurs, the former is also no longer accorded with the experimental curve.

Fig. 11 (c) indicates the curves at 12 in. (near-exit) of total heated length in Section 4. In this case, when the decomposition occurs, the experimental curve transits from the proposed relation curve due to near-inlet condition (at 1 in.; $Nu^* = 1.55$) to near-exit condition (at 13 in.; $Nu^* = 1.83$). In this case, unlike in the case at 9 in., experimental Nusselt number curve exists between $Nu^* = 1.55$ and 1.83 from the decomposition beginning to end, in spite of coking formation reduced it.

Fig. 12 shows the curves at 12 in. (near-exit) of total heated length in Section 5 of large heat flux case. In this case, when the decomposition occurs, the experimental curve exists between Nusselt numbers due to near-inlet and near-exit conditions approximately; or transits from the former to the latter. After large coking formation starts, they are no longer accorded with the reduced curve.

By these results, it may be applicable for the evaluation of the enhanced Nusselt number due to endothermic reactions in developed turbulent flows, such as in the regenerative cooling passages; except that the reduction related to coking formation which occurs at the wall surface due to huge heat flux, as shown in Fig. 12. Therefore, In other words, it can be

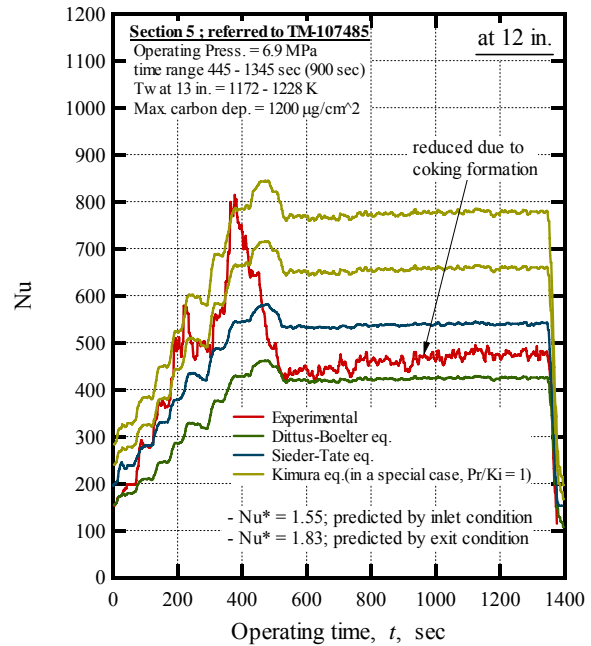


Fig. 12 The comparison result of overall Nusselt numbers between experimental value (TM-107485¹²⁾) and some correlated equation values; Test Section 5 (with large heat flux): Haynes 230, at 12 in. (near-exit) of total heat length of 14 in.

concluded that if the wall temperature, mean bulk fluid temperature, and heat sink characteristics (temperature dependence as shown in Fig. 1 or 9) are known or can be predicted, enhanced Nusselt number is predictable.

(iv) Effect of Corking Formations due to Large Heat Flux

As mentioned above, the proposed relation equation is not applicable when the large coking formation occurs at the wall surface of coolant channels as shown in Fig. 12. However, such applicability is not indispensable. It is because, according to Boudreau¹⁶⁾, the practical limit of endothermic cooling application is coking limit of the fuel, from the perspective of the reusability of the coolant channels.

Conclusions

In this paper, a new relation expression equation was proposed by classical theoretical approaches. It provides the prediction of the enhanced Nusselt number related to the endothermic reactions due to heterogeneous chemical decompositions in developed turbulent forced-convective flows such as in the regenerative cooling passages. It allows that the prediction of that without investigation of the detailed reaction mechanisms.

Evaluation of validity and applicability of the proposed equation was also carried out by comparison to the results of heated tube tests using supercritical JP-7 fuel carried out at NASA Lewis Research Center.

Its non-dimensional specific heat ratio was estimated by the temperature dependence of its chemical heat sink characteristics evaluated by UTRC.

As a result, it has been suggested that the proposed equation may be applicable to the prediction of Nusselt number enhancement due to such chemical reactions except when comparatively large coking formation occurs. Aiming to practical use of the proposed equation, further evaluation of its validity and applicability, and investigations into the correlations between Γ_p value and type of fuels are required.

Nomenclatures

Alphabetic Letters

- A : Area, m^2
 $c_{p,\xi}$: Specific heat related to temperature change at constant pressure, J/kgK
 $c_{v,\xi}$: Specific heat related to temperature change at constant volume, J/kgK
 h : Specific enthalpy, J/kg
 h_{ref} : Specific enthalpy at the temperature of T_{ref} , J/kg
 h_w : Specific enthalpy at the temperature of T_w , J/kg
 $h_{p,T}$: Specific heat related to chemical change at constant pressure, J/kg-mol
 Δh : Specific enthalpy difference due to ΔT and $\Delta\xi$, J/kg
 Δh_w : Specific enthalpy difference due to ΔT_w and $\Delta\xi_w$, J/kg
 $\Delta h_{chem,w}$: Specific enthalpy difference due to $\Delta\xi_w$, J/kg
 $\Delta h_{phys,w}$: Specific enthalpy difference due to ΔT_w , J/kg
 $N_{p,j}$: Amount of substance of product j , mol
 $N_{R,i}$: Amount of substance of reactant i , mol
 p : Pressure of Fluid, Pa
 q_y^{chem} : Heat flux related to chemical change, W/m^2
 q_y^{phys} : Heat flux related to temperature change, W/m^2
 q_y^{total} : Total heat flux, W/m^2
 Q_y^{chem} : Heat flow related to chemical change, W
 Q_y^{phys} : Heat flow related to temperature change, W
 Q_y^{total} : Total heat flow, W
 T : Temperature, K
 T_b : Bulk temperature of fluid, K
 T_{ref} : Reference temperature of fluid, K
 T_w : Wall temperature, K
 \bar{T} : Time averaged temperature of T , K
 T' : Turbulent-induced fluctuation of temperature of T , K
 ΔT : Difference between the temperatures of T and T_{ref} , J/kg
 ΔT_w : Difference between the temperatures of T_w and T_{ref} , J/kg
 u : Velocity of fluid in x direction, m/s
 v : Velocity of fluid in y direction, m/s
 \bar{v} : Time averaged velocity of v , m/s

- v' : Turbulent-induced fluctuation of velocity of v , m/s
 x : Coordinate in convective flow direction, m
 y : Distance from the wall surface, m
 Y : Distance, m

Greek Letters

- α_{phys} : Heat transfer coefficient, W/m^2K
 α_{total} : Total heat transfer coefficient, W/m^2K
 γ_ξ, Γ_ξ : Ratio of specific heat at constant extent of reaction, -
 Γ_p : Ratio of specific heat at constant pressure, -
 $\nu_{p,j}$: Stoichiometric coefficient of product j , -
 $\nu_{R,i}$: Stoichiometric coefficient of reactant i , -
 ρ : Density of fluid, kg/m^3
 ξ : Extent of reaction, mol
 ξ_w : Extent of reaction of fluid at wall surface, mol
 ξ_{ref} : Reference extent of reaction of fluid, mol
 $\bar{\xi}$: Time averaged extent of reaction of ξ , mol
 ξ' : Turbulent-induced fluctuation of extent of reaction of ξ , mol
 $\Delta\xi$: Difference between the extent of reactions of ξ and ξ_{ref} , J/kg
 $\Delta\xi_w$: Difference between the extent of reactions of ξ_w and ξ_{ref} , J/kg

Transport Properties

- κ : Coefficient of molecular chemico-thermal conductivity of fluid, $W/m\text{-mol}$
 κ^{turb} : Coefficient of turbulent chemico-thermal conductivity of fluid, $W/m\text{-mol}$
 λ : Coefficient of molecular physico-thermal conductivity of fluid, W/mK
 λ^{turb} : Coefficient of turbulent physico-thermal conductivity of fluid, W/mK
 μ : Coefficient of molecular viscosity of fluid, Pa-s
 μ^{turb} : Coefficient of turbulent viscosity of fluid, Pa-s
 ν : Kinematic coefficient of molecular viscosity
 ν^{turb} : Kinematic coefficient of turbulent viscosity, m^2/s
 a_κ : Coefficient of chemico-thermal diffusivity related to temperature change, m^2/s
 a_λ : Coefficient of physico-thermal diffusivity related to chemical change, m^2/s
 a_κ^{turb} : Coefficient of turbulent chemico-thermal diffusivity related to temperature change, m^2/s
 a_λ^{turb} : Coefficient of turbulent physico-thermal diffusivity related to chemical change, m^2/s

Non-dimensionalized parameters

- Nu^* : Ratio of Nusselt numbers Nu_{total} to Nu_{phys}
 $c_{p,\xi}^*$: Dimensionless specific heat of $c_{p,\xi}$
 $c_{v,\xi}^*$: Dimensionless specific heat of $c_{v,\xi}$
 $h_{p,T}^*$: Dimensionless specific heat of $h_{p,T}$
 h^* : Dimensionless enthalpy of h
 h_w^* : Dimensionless enthalpy of h_w

- T^* : Dimensionless temperature of T
 T_w^* : Dimensionless temperature of T_w
 ξ^* : Dimensionless extent of reaction of ξ
 ξ_w^* : Dimensionless extent of reaction of ξ_w
 y^* : Dimensionless coordinate of y

Non-dimensional Numbers

- Nu_{DB} : Nusselt number evaluated by Dittus-Boelter's correlation equation
 Nu_{phys} : Normal Nusselt number
 Nu_{total} : Total Nusselt number
 Re : Reynolds number
 Pr : Molecular Prandtl number
 Pr^{turb} : Turbulent Prandtl number
 Ki : Tentatively defined non-dimensional number for molecular transport of heat of reaction
 Ki^{turb} : Tentatively defined non-dimensional number for turbulent transport of heat of reaction

References

- 1) Lander, H., Nixon, A.C.: Endothermic Fuels for Hypersonic Vehicles, *J. Aircraft*, Vol.8, No.4, Apr. 1981, pp. 200-207.
- 2) Petley, D.H., Jones, S.C.: Thermal Management for a Mach 5 Cruise Aircraft Using Endothermic Fuel, *J. Aircraft*, Vol.29, No.3, 1992, pp. 384-389.
- 3) Glickstein, M.R., Spadaccini, L.J.: Applications of Endothermic Reaction Technology to the High Speed Civil Transport, NASA CR-207404, Apr. 1998.
- 4) Powell, O.A., Edwards, J.T., Norris, R.B., Numbers, K.E., Pearce, J.A.: Development of Hydrocarbon-Fueled Scramjet Engines: The Hypersonic Technology (HyTech) Program, *J. Propulsion and Power*, Vol.17, No. 6, Nov.-Dec. 2001, pp.1170-1176.
- 5) Edwards, T.: Liquid Fuels and Propellants for Aerospace Propulsion: 1903-2003, *J. Propulsion and Power*, Vol.19, No.6, Nov.-Dec. 2003, pp.1089-1107.
- 6) Huang, H., Spadaccini, L.J., Sobel, D.R.: Fuel-Cooled Thermal Management for Advanced Aeroengines, *J. Eng. Gas Turbines Power*, Vol. 126, Apr. 2004, pp. 284-293.
- 7) Huber, M.L.: NIST Standard Reference Database 4, NIST Thermophysical Properties of Hydrocarbon Mixtures Database (SUPERTRAPP) Ver. 3.1.
- 8) Schlichting, H. and Gersten, K.: *Boundary-Layer Theory*, 8th ed., Springer-Verlag, Germany, 2000, pp. 237-240.
- 9) Masters, P.A., Aukerman, C.A.: Deposit Formation in Hydrocarbon Rocket Fuels with an Evaluation of a Propane Heat Transfer Correlation, NASA TM-82911, Jun. 1982.
- 10) Giovanetti, A.J., Spadaccini, L.J., Szetela, E.J.: Deposit Formation and Heat-Transfer Characteristics of Hydrocarbon Rocket Fuels, *J. SPACECRAFT*, Vol.22, No.5, pp. 574-580.
- 11) Prigogine, I., Kondepudi, D.K.: MODERN THERMODYNAMICS: From Heat Engines to Dissipative Structures, John Wiley & Sons, New York, 1998, pp. 57-59, 110.
- 12) Linne, D.L., Meyer, M.L., Edwards, T., Eitman, D.A.: Evaluation of Heat Transfer and Thermal Stability of Supercritical JP-7 Fuel, NASA TM-107485, Jul. 1997.
- 13) Bird, R.B., Stewart, W.E., and Lightfoot, E.N.: *Transport Phenomena*, 2nd ed., John Wiley & Sons, New York, 2002, pp. 266-267.
- 14) Holeman, J.P.: *HEAT TRANSFER*, 4th ed., McGraw-Hill Kogakusha, Tokyo, 1976, pp.204, 206.
- 15) Meyer, M.L.: Electrically Heated Tube Investigation of Cooling Channel Geometry Effects, NASA TM-106985 (AIAA-95-2500), Jun. 1995.
- 16) Boudreau, A.H.: STATUS OF THE U.S. AIR FORCE HYTECH PROGRAM, AIAA 2003-6947, 12th AIAA International Space Planes and Hypersonic Systems and Technologies, Dec. 2003, Norfolk, Virginia.